Supplementary Material (ESI) for Chemical Communications

Electronic Supplementary Information

CO_2 Selectivity of a 1D Microporous Adenine-Based Metal Organic Framework Synthesised in Water

Kyriakos C. Stylianou, John E. Warren, Samantha Y. Chong, Jeremy Rabone, John Bacsa, Darren Bradshaw and Matthew J. Rosseinsky†

† Department of Chemistry, University of Liverpool, Liverpool L69 7ZD, UK

Table of Contents

1. Synthesis, Crystal Data and Structure Representation

Synthesis of $[Ni_3(pzdc)_2(7Hade)_2(H_2O)_4]\cdot(H_2O)_{1.5}$ (**1**)*:*

A mixture of $NiCO_3$ (48 mg, 0.40 mmol), 3,5-pyrazoledicarboxylic acid, H_3pzdc (47 mg, 0.30 mmol), adenine, 9Hade (40 mg, 0.30 mmol), and water (8 mL) was placed in a 20 mL Teflon reactor. The mixture was stirred for 10 min at room temperature. The initial pH of the blue solution was 5.8. The reactor was heated at 140 °C for 72 hours, and then cooled to room temperature at a rate of 0.1 ºC / min. The final pH of the reaction was 5.4. Blue needle-like crystals of **1** were obtained and were washed with H_2O. Yield: 52% based on $NiCO_3$. Anal. Calcd for ($Ni_3C_{20}N_{14}O_{13.5}H_{23}$) : C 28.20, H 2.72, N 23.02. Experimental : C 28.37, H 2.89, N 23.12. Outside the specified pH range, impurities, such as free 9Hade and a nickel pyrazolate coordination polymer, are present in the bulk product. The guest H_2O content is lower than that refined from the single crystal data of 2.18, as the crystals were measured directly from the mother liquor whereas the bulk material for microanalysis was filtered.

Desolvation procedure of **1**:

Blue **1** was outgassed at 60 ºC under dynamic vacuum (10^{-5} mbar) overnight to yield purple **1′** indicating a possible change in the coordination environment around the three metal ions upon full desolvation. This colour change is also observed by TGA analysis at 230 °C, where a mass loss of 12.1% corresponds to loss of all guests – O3W and O4W – and coordinated solvent, O1W and O2W. The formula of **1′** was determined by elemental analysis as $Ni_3(pzdc)_2(7Hade)_2(H_2O)_{0.6}$ (Anal. Calcd : C 31.47, H 1.79, N 25.69, Experimental: C 31.28, H 2.01, N 25.76) (The 0.6 water content for the samples prepared for CHN analysis most likely arises from adventitious contaminantion by atmospheric water incurred during analysis. The TGA data and PXRD data show a stable water-free phase at high temperature)

When purple **1′** is exposed to the atmosphere the blue colour of **1** is regenerated within few minutes, attributed to the reversible coordination of atmospheric H_2O molecules to Ni(II).[1] The formula of the re-hydrated **1″** was also determined by elemental analysis as $[Ni_3(pzdc)_2(7Hade)_2(H_2O)_4]\cdot(H_2O)_{0.4}$ (Anal. Calcd : C 28.88, H 2.52, N 23.57. Experimental: C 28.92, H 2.59, N 23.64.) The reversibility of the hydration/dehydration is further confirmed by PXRD. All figures and PXRD justifying the above characterisation and observations are shown below.

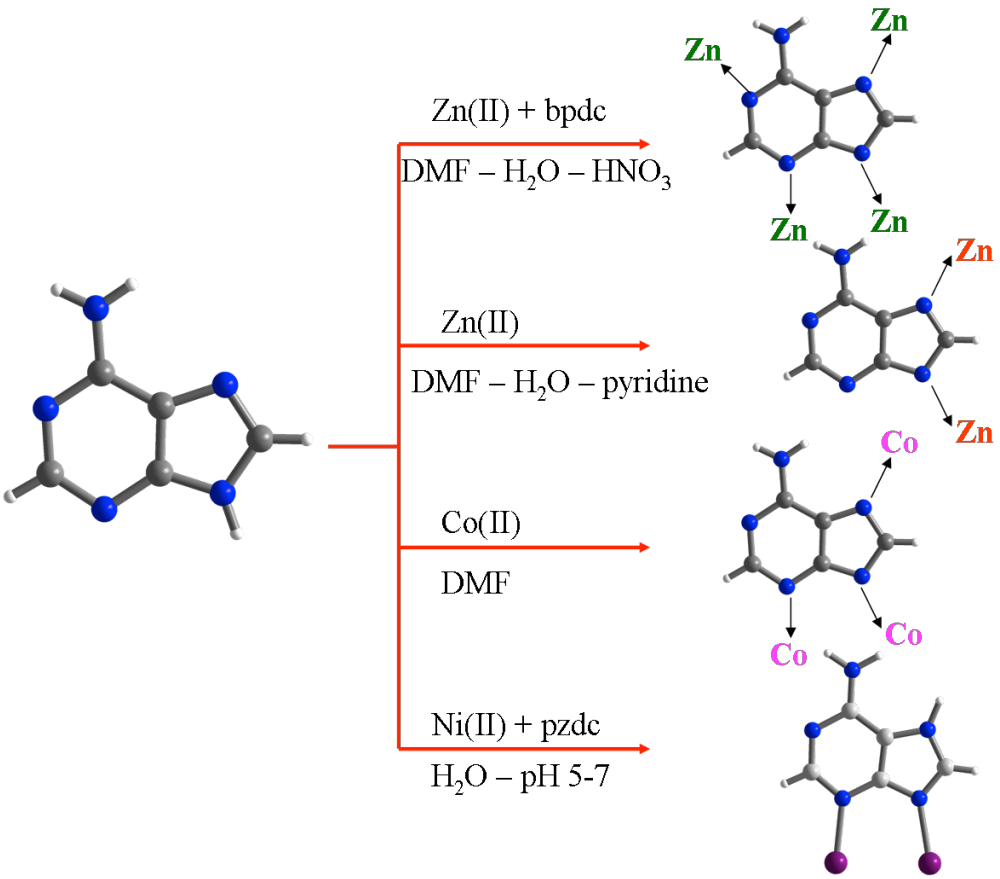

Scheme S1: Reaction conditions and different coordination modes of adenine in MOFs reported in the literature and the material reported here, bottom.[2-4] (C : grey, N : nitrogen, H : white and Ni : purple)

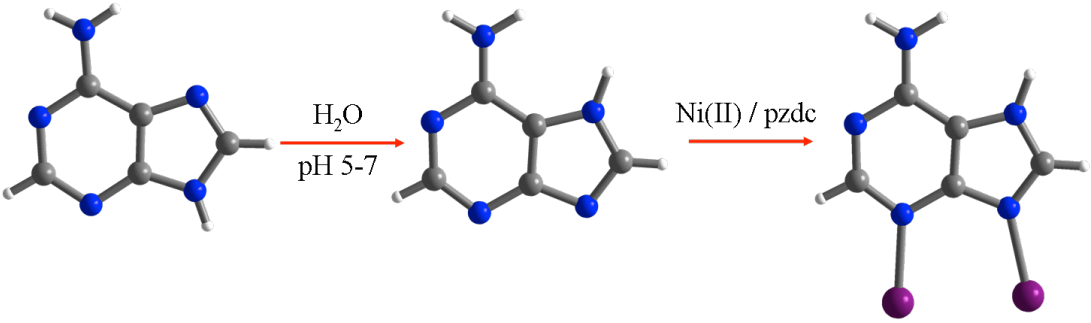

Scheme S2: Migration of the H atom between the imidazolate N atoms and selective deprotonation of adenine required to form the bidentate mode – from N3 and N9 (C : grey, N : nitrogen, H : white and Ni : purple).[5]

Structure representation

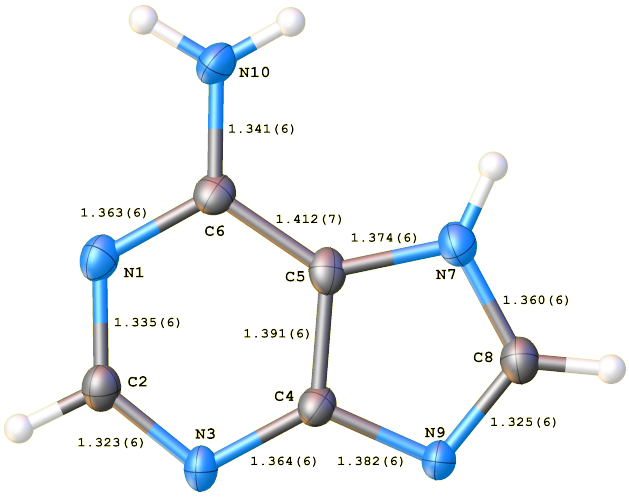

Figure S1 : Diagram of 7Hade bond lengths in **1**

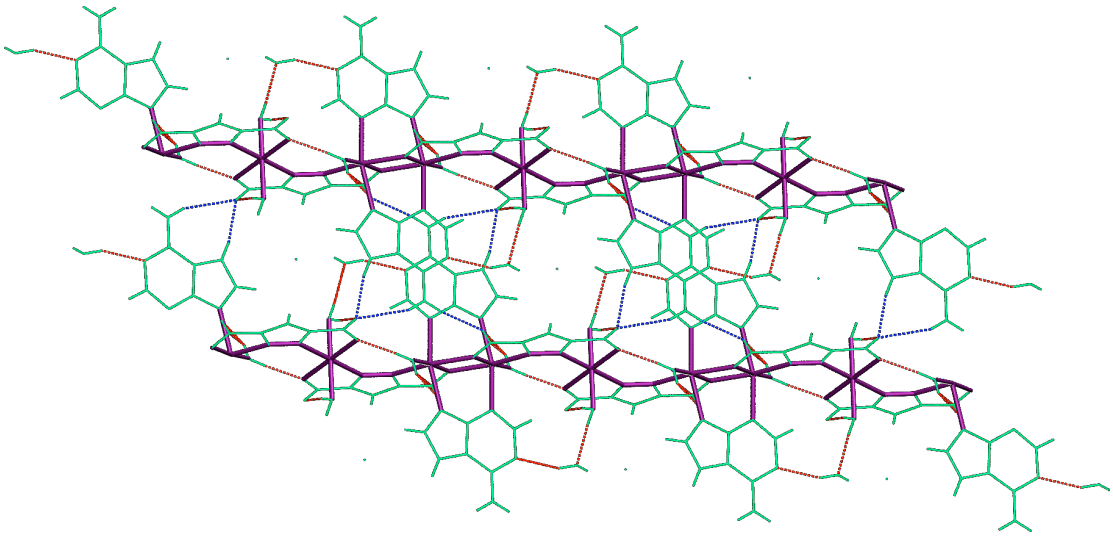

Figure S2 : Depiction of the hydrogen bonding network in **1** which links the 1-D chains (view down a-axis). First coordination sphere of Ni sites shown in purple, ligand framework and water shown in green. Blue dotted line indicates hydrogen bond originating from nitrogen, red from oxygen.

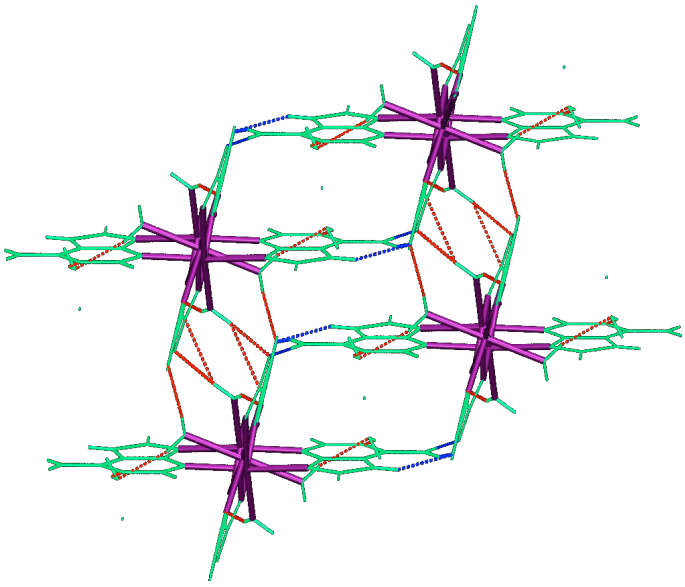

Figure S3 : Depiction of hydrogen bonding network, linking between 1-D chains (view down c-axis). First coordination sphere of Ni sites shown in purple, ligand framework and water shown in green. Blue dotted line indicates hydrogen bond originating from nitrogen, red from oxygen.

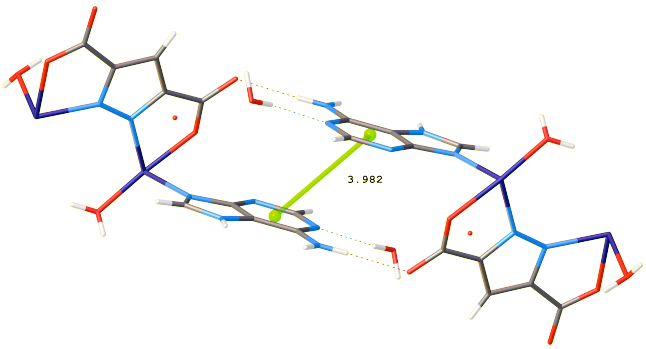

Figure S4 : Depiction of centroid-centroid distance and shift displacement (green) between two 7Hade rings showing π – π interaction within conventional π – π stabilisation distance.

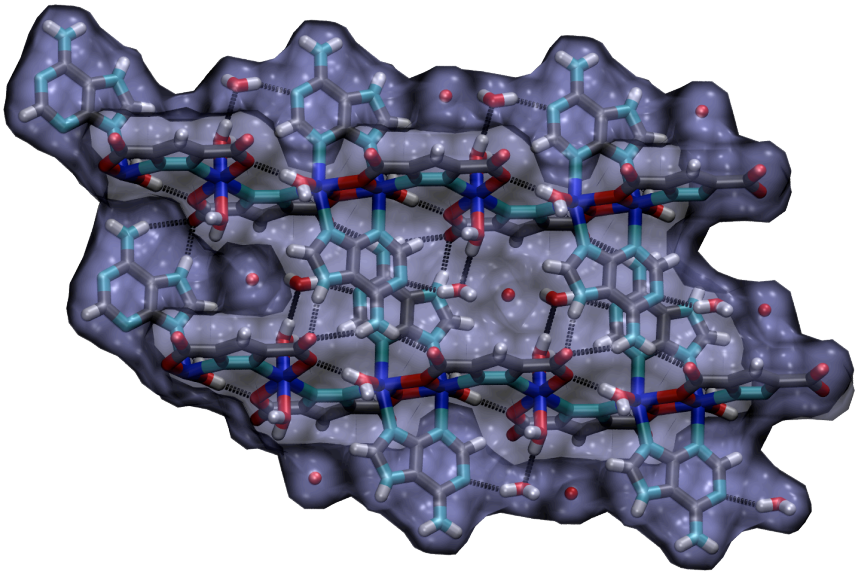

Figure S5: MSMS molecular surfaces generated with a probe radius of 1.2 Å for the fully solvated structure of **1**, hydrogen bonding shown as black dashed lines.

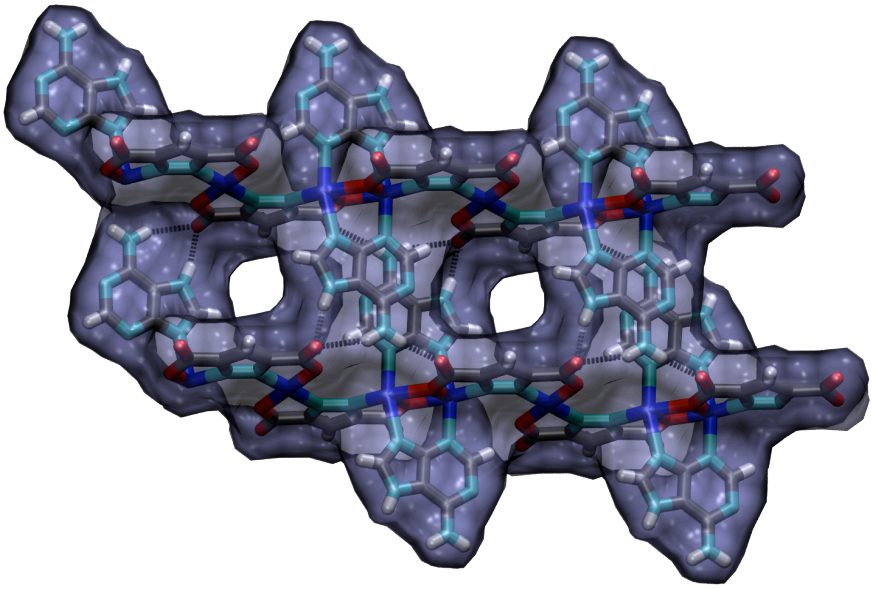

Figure S6 : MSMS molecular surfaces generated with a probe radius of 1.2 Å for **1** with all the water removed, hydrogen bonding shown as black dashed lines.

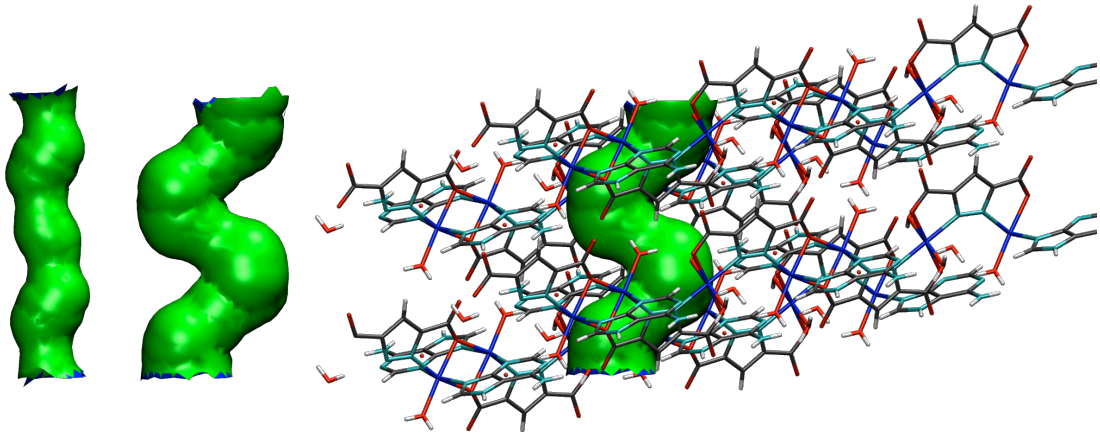

Figure S7 : Hole2 channel surfaces showing cavity shape for removal of unbound water, O3W, O4W (left) from **1** and fully desolvated with all metal-bound water, O1W, O2W removed (middle). Depiction of fully desolvated channel in the as-made framework (right). Water accessible parts (1.15 Å > pore radius < 2.30 Å) are green and wide areas (pore radius > 2.30 Å are blue). View chosen to place channel flat to plane of paper comparable to view down 010 direction.

Crystal structure determination

Single crystals of **1** were synthesized from hydrothermal synthesis mounted in Fomblin inert oil on a two stage capillary fibre and transferred to the cold gas stream (150 K) of the Bruker-Nonius APEXII CCD diffractometer. Single-crystal diffraction data was collected at Station 9.8 of the SRS, Daresbury Laboratory, at a wavelength of 0.6939 Å. A hemisphere of data was collected at 0.36° scan widths and one second uncorrelated exposure times. The index data proved not to be a single crystal. Subsequent deconvolution isolated two dominant domains with no obvious relating twin law. Two orientation matrices where determined and the sample integrated as a twin using SAINT.[6] The structure present here is from a single domain of the twinned data and refined as a single domain after integration (SAINT) and scaling (TWINABS[7]) as a two domain system. This proved to provide the best R-factor and cleanest difference map. Refinements on the second domain and using the combined data treated as a twin both proved to give lower quality models with larger residual electron density. The final structure was solved using Olex2[8] superflip[9] and refined using SHELX-97.[10]

Brief:

Crystal Data. $C_{20}H_{24}N_{14}O_{14.18}Ni_3$, M =863.54, Triclinic, a = 7.332(5) Å, b = 9.916(6) Å, c = 11.832(7) Å, α = 67.278(8)°, β = 80.572(9)°, γ = 72.566(8)°, U = 755.9(8) Å^3, T = 150.0 K, space group P-1 (no. 2), Z = 1, μ(Synchrotron) = 1.943, 3698 reflections measured, 3026 unique (Rint = 0.1289) which were used in all calculations. The final wR(F2) was 0.1218 (all data).

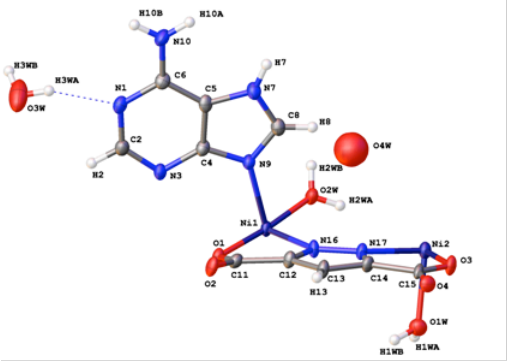

Asymmetric Unit

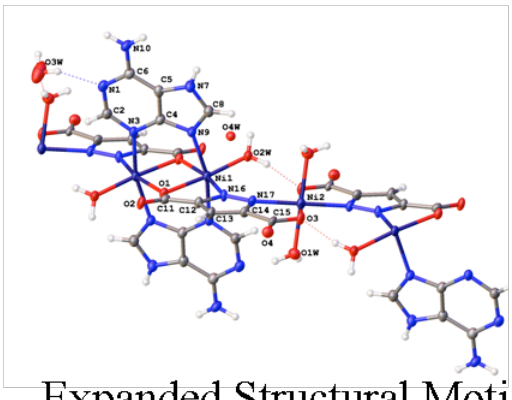

Expanded Structural Motif

Empirical formula	$C_{20}H_{24}N_{14}O_{14.18}Ni_3$
Formula weight	863.54
Temperature / K	150
Crystal system	Triclinic
Space group	P-1
a / Å	7.332(5)
b / Å	9.916(6)
c / Å	11.832(7)
α/°	67.278(8)
β/°	80.572(9)
γ/°	72.566(8)
Volume / $Å^3$	755.9(8)
Z	1
ρ_{calc} / mg mm^{-3}	1.897
μ / mm^{-1}	1.943
F(000)	439
Crystal size / mm^3	0.1 × 0.02 × 0.01
Theta range for data collection	2.34 to 25.70°
Index ranges	$-7 \le h \le 9$, $-9 \le k \le 12$, $-14 \le l \le 14$
Reflections collected	3698
Independent reflections	3026
R(int) =	0.129
Data/restraints/parameters	3026/11/252
Goodness-of-fit on F^2	0.936
Final R indexes [I>2σ (I)]	$R_1 = 0.0493$, $wR_2 = 0.1122$
Final R indexes [all data]	$R_1 = 0.0937$, $wR_2 = 0.1218$
Largest diff. peak/hole / e $Å^{-3}$	0.639/-0.908

Table S1 : Hydrogen Bonding Donor Acceptor Distances and Angles

H-bonds	d(D-A)/Å	D-H-A/°
Intramolecular		
O2W···O3*	2.643(5)	163(4)
Intermolecular		
O2W···O2	2.742(5)	158(4)
O1W···O4	2.932(5)	168(5)
N10···O2*	2.962(5)	172.1(5)
N10···O4*	3.235(6)	155.5(5)
N7···O4	2.758(5)	155.4(5)
O3W···N	2.821(6)	157(8)
O1W···O3W	2.765(6)	166(4)

* Shown in figure 1b.

Table S2 : Olex2 CalcVoid Analysis 0.1 Å Resolution in Precise Mode

State	Penetration Sphere Radius Å			Cell Volume Å^3	Radius Largest Spherical Void Å	Structure Occupancy	
	a	b	c			Å^3	%
Fully Solvated	0.40	0.30	0.30	755.88	1.20	537.49	71.11
Channel Partial Desolvated	0.80	0.30	0.30	755.88	1.30	523.09	69.20
Channel Desolvated - O3W, O4W$^{\infty}$	1.20	0.30	0.30	755.88	1.70	492.62	65.17
Pendant Desolvated -O2W	1.20	0.40	0.40	755.88	1.70	468.89	62.03
Fully Desolvated - O1W, O2W, O3W, O4W	1.20	0.40	0.40	755.88	2.10	440.95	58.34

∞ The solvent accessible volume calculated from Platon is 12.1% per unit cell with a packing index of 66.6%. This is greatly larger than the 2.72% calculated from conversion of the largest spherical void from Olex2 due to the different methods utilised by Olex2 and Platon to calculate accessible space. Olex2 only looks for the largest single void space a sphere can occupy to provide the largest spherical void space (this is per instance and not multiplied by symmetry for the cell) where as Platon uses a merged overlapping sphere model. The occupied volume or packing index calculated from Platon is also slightly larger than in Olex2. This is because Platon utilises a greater radii (1.20 Å) for hydrogen atoms. With the equivalent hydrogen radii Olex2 gives 66.60% occupied volume. We feel both figures have merit in understanding the void space of these materials.

Element Radii

Element	Radii
C	1.7
H	1.09
N	1.55
Ni	1.63
O	1.52
Default radii source: http://www.ccdc.cam.ac.uk/products/csd/radii	

2. Powder X-ray Diffraction (PXRD)

Powder X-ray diffraction data of **1**, **1′** and *in situ* Variable Temperature (VT) PXRD on **1** sealed in a capillary were collected at station I11 of the Diamond Synchrotron, U.K., at a wavelength of 0.82633 Å. **1′** was prepared by outgasing **1** under high vacuum (10^{-5} mbar) overnight and the capillary was sealed under inert conditions.

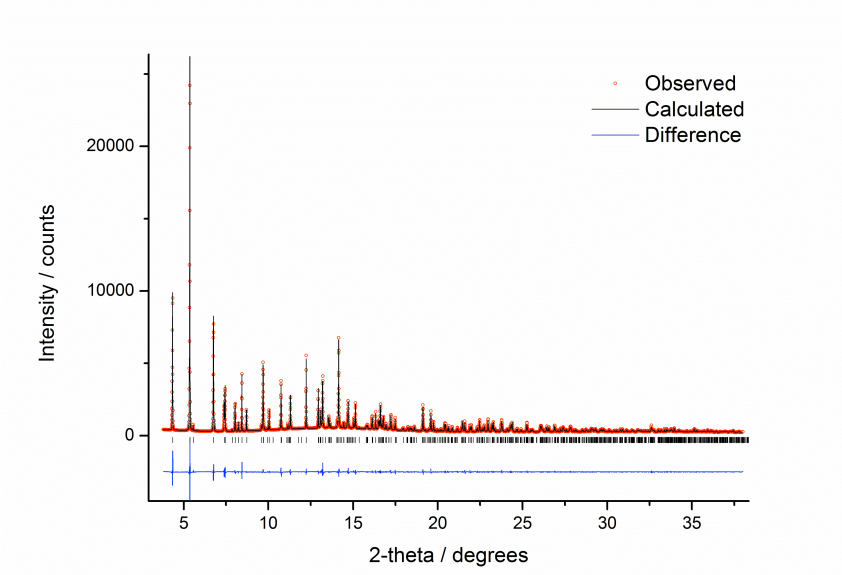

Figure S8 : Final observed (circles), calculated (solid lines) and difference (below) X-ray diffraction for the Le Bail refinements of **1** (Rwp = 4.92 %, Rp = 3.43 %, χ^2 = 5.87, $P\bar{1}$; a = 7.349 Å, b = 9.910 Å, c = 11.800 Å, α = 67.293 º, β = 80.670 º and γ = 72.428º, V = 754.94 $Å^3$) consistent with the cell obtained from single crystal data. Reflection positions are marked.

3. Thermo Gravimetric Analysis (TGA) of 1

Thermo gravimetric analyses were performed under N_2 atmosphere using a SEIKO S – II instrument. The heating rate was 5 ºC / min until 600 ºC and then cooled to room temperature at a rate of 10 ºC / min.

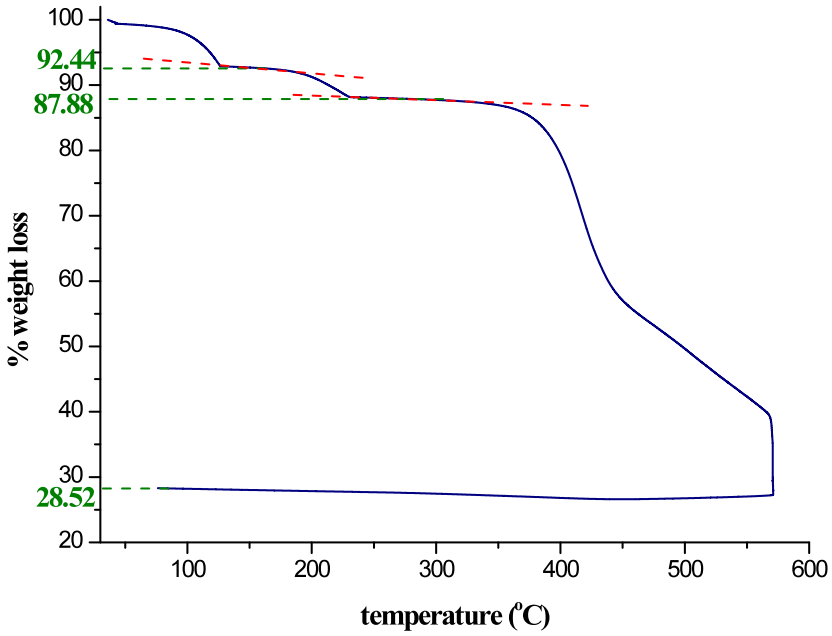

Figure S9: TGA of **1** showing that the first weight loss (~7.5 %) corresponds to 3.5 H_2O molecules – 1.5 guests (O3W and O4W) and 2 coordinated (O1W) – and the second loss is due to the loss of the remaining 2 coordinated H_2O molecules (O2W). The framework is stable up to 380 ºC.

4. Infrared Spectroscopy

The IR spectra of H_3pzdc, 9Hade and **1** were recorded on Perkin Elmer instrument Spectrum 100.

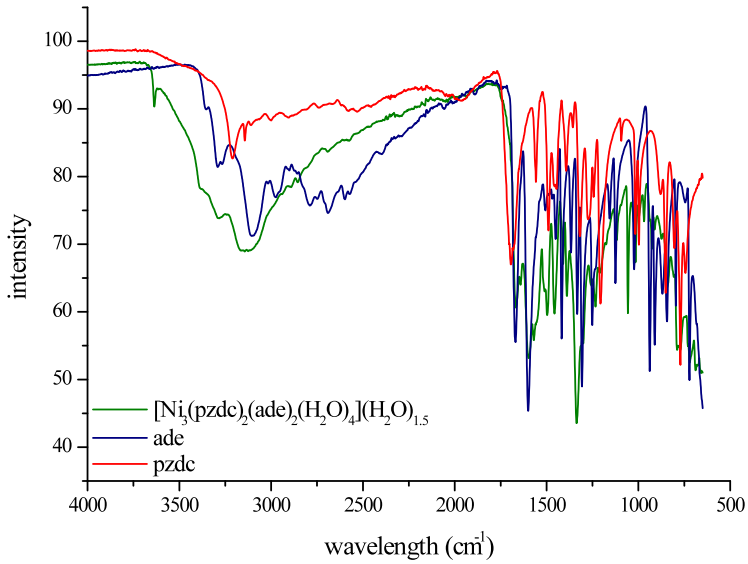

Figure S10 : IR spectra of **1** and free H_3pzdc and 9Hade. The N-H band of the free H_3pzdc at 3189 cm^{-1} is not present in the as made material confirming the coordination of N to Ni. The N-H bands for adenine are present in the region of 2750 – 3500 cm^{-1}, showing the coordination of adenine in **1**.

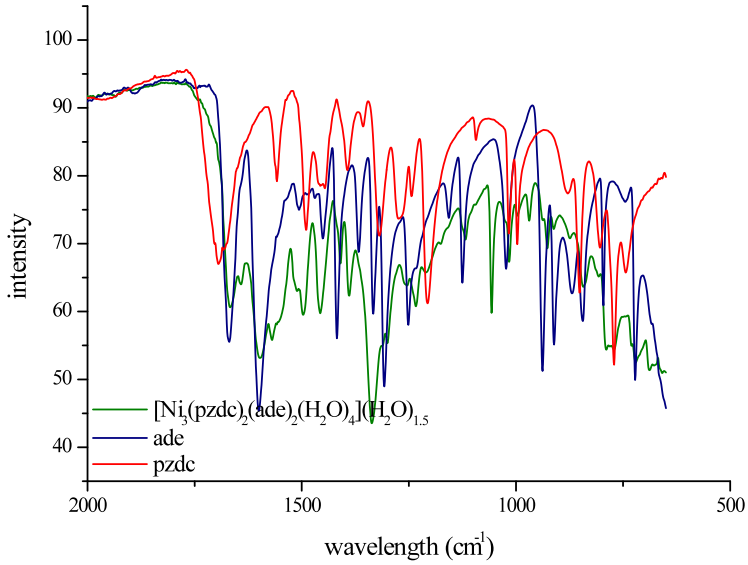

Figure S11 : IR spectra at the region between 550 – 2000 cm^{-1}. The shift of the C=O band of the free H_3pzdc at 1658 cm^{-1} confirms its coordination to nickel.

5. PXRD of desolvated material

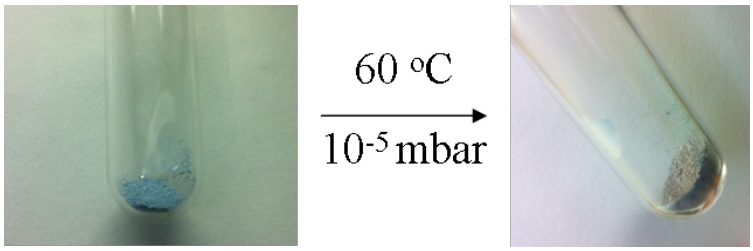

Figure S12 : The colour of the material turns from blue (**1**) to purple (**1′**) upon desolvation.

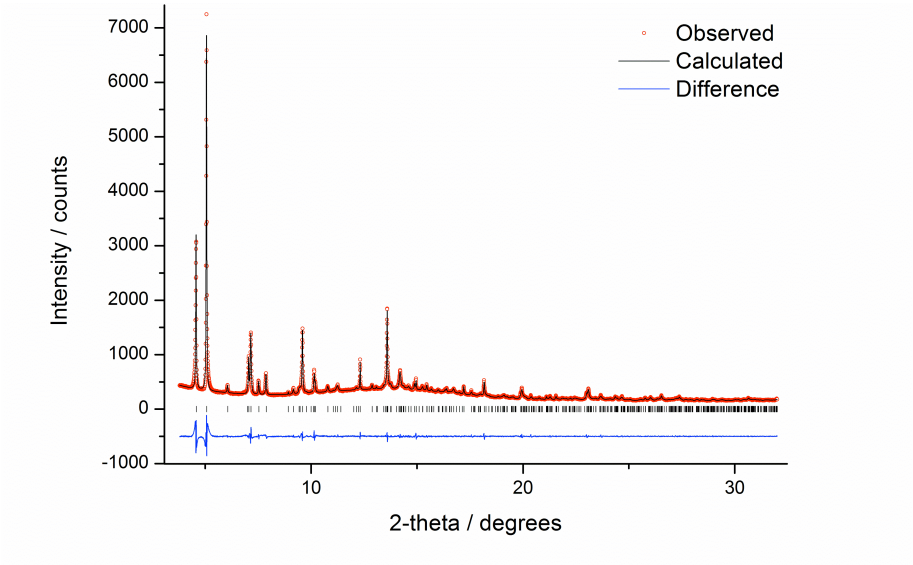

Figure S13 : Final observed (circles), calculated (solid lines) and difference (below) X-ray diffraction for the Le Bail refinements of **1′** (Rwp = 4.84 %, Rp = 2.89 %, χ^2 = 4.81, $P\bar{1}$; a = 7.437 Å, b = 10.049 Å, c = 10.898 Å, α = 97.191 º, β = 76.263 º and γ = 72.011 º, V = 735.00 Å^3). Reflection positions are marked.

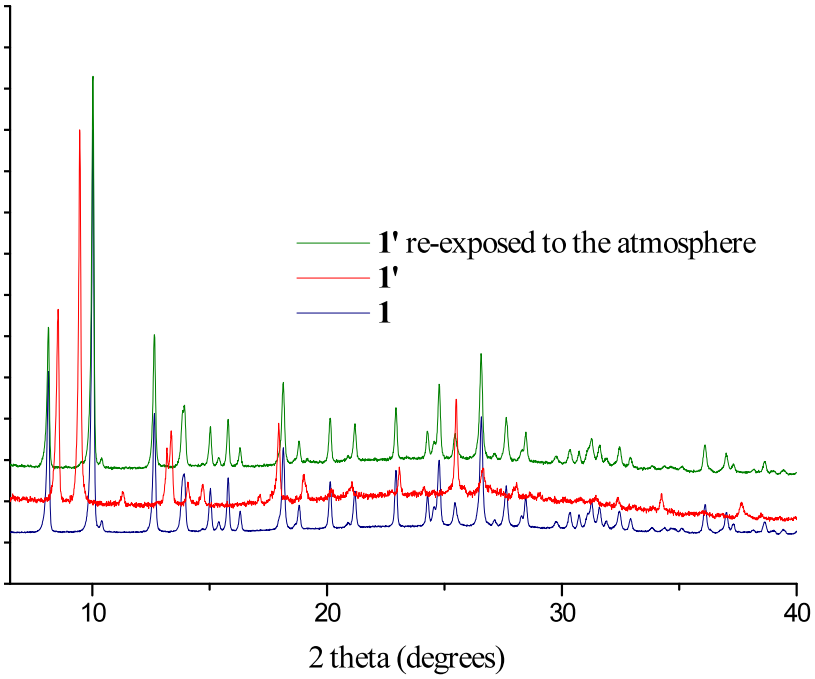

Figure S14: Comparison of the PXRD patterns of **1** and **1′** and **1′** after exposure to the atmosphere.

Variable Temperature PXRD :

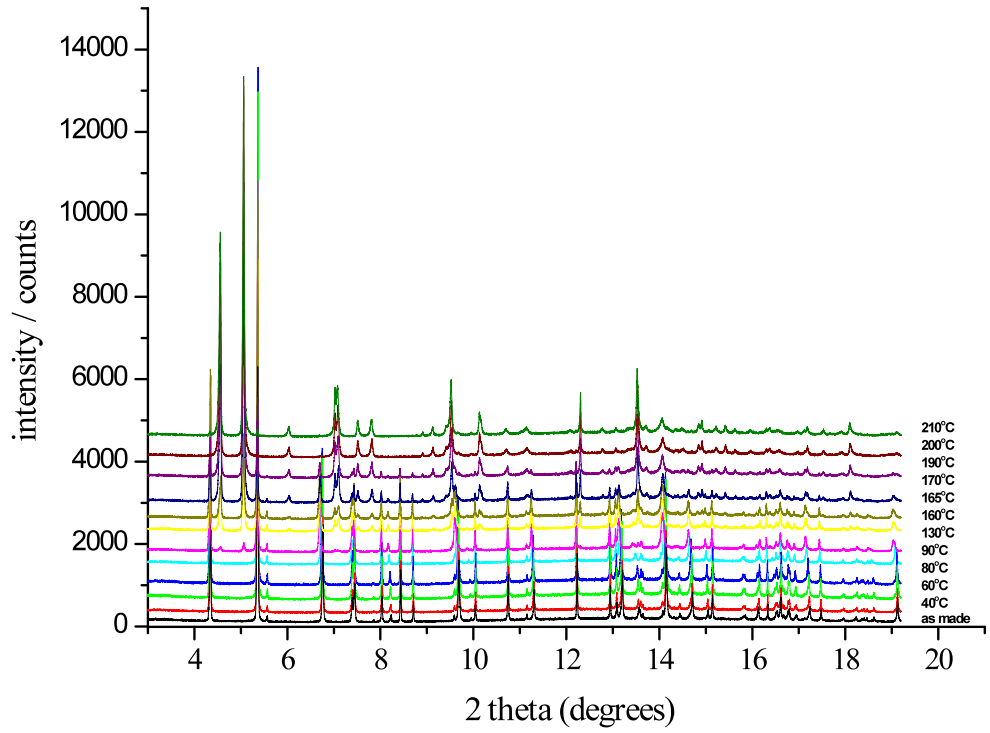

Figure S15 : Variable Temperature PXRD of **1** which shows that **1** is stable up to 80 ºC. Between 80-165 ºC both **1** and **1′** are present. Above 165 ºC only **1′** is present.

6. Sorption Study and Isosteric heat

High purity CO_2 (99.995 %), N_2 (99.99 %) and CH_4 (100 %) were purchased from BOC gases and used as received. All sorption isotherms were measured using the Intelligent Gravimetric Analyser (IGA) from Hiden. **1** was washed with H_2O and dried in a dessicator under vacuum overnight. **1** was activated by outgassing at 60 ºC under ultra high vacuum (10^{-6} mbar) overnight. The carbon dioxide measurements were performed at 195 K and 1 bar and at 273 K and 298 K at 5 bar. CH_4 isotherms were also collected at 273 K and 298 K at 1 and 5 bar. Finally, nitrogen isotherms were collected at 77 K and 1bar.

BET plot of CO_2 adsorption

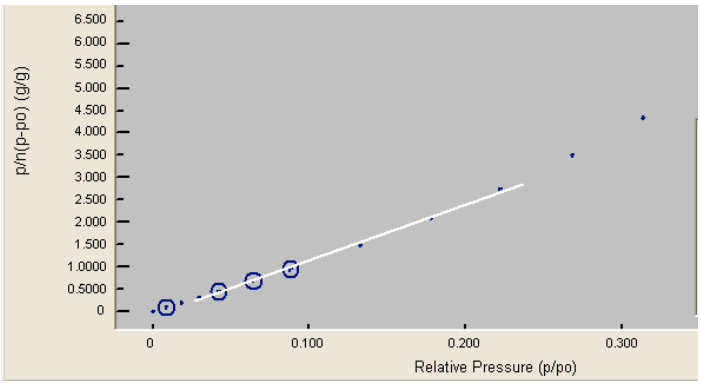

Figure S16 : Plot of the linear region for the BET equation in the range below p/p^0 0.24.

DR equation

The CO_2 isotherm was studied using the Dubinin – Radushkevich (DR) equation to characterise the porosity of **1′** .

$$\log V = \log Vo - \frac{RT}{\beta Eo}\left(\log \frac{p^0}{p}\right)^2$$

Where: V = volume adsorbed at equilibrium pressure (cm^3/g),

Vo = the micropore capacity (cm^3/g),

p^0 = saturation vapor pressure of gas at temperature T,

p = equilibrium pressure,

β = the affinity coefficient of analysis gas relative to Po gas (β is taken to be 1),

T = temperature (77.4K)

R = gas constant 8.314 KJ/mol

Eo = activation energy (KJ/mol)

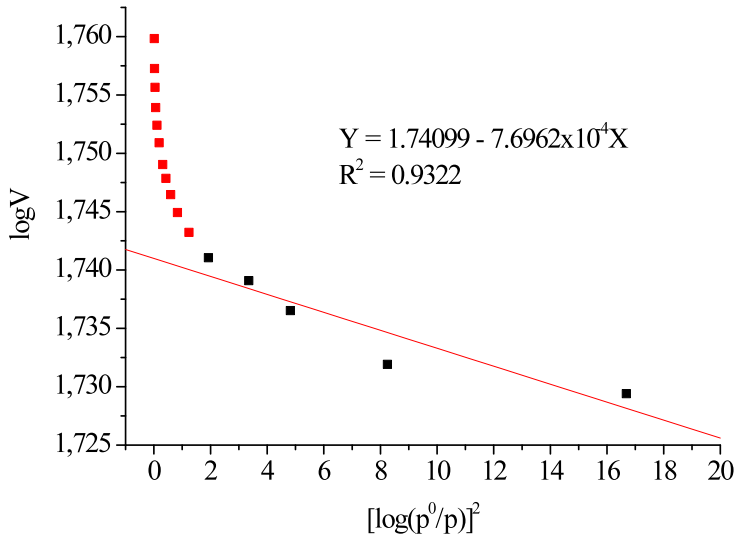

Figure S17 : Plot of DR equation (for CO_2 isotherm collected at 195K and 1 bar) of $\log V = f[(\log p^0/p)^2]$

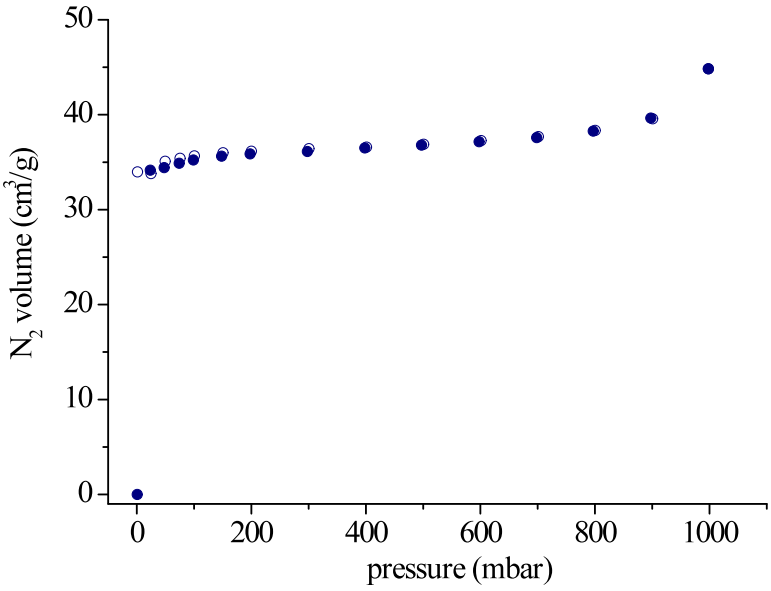

Figure S18 : Nitrogen isotherm collected at 1 bar and 77 K. The application of the BET model in the relative pressure of p/p^0 0.02-0.22, results in a surface area of 124.4 ± 3.4 m^2/g.

BET plot of N_2 adsorption

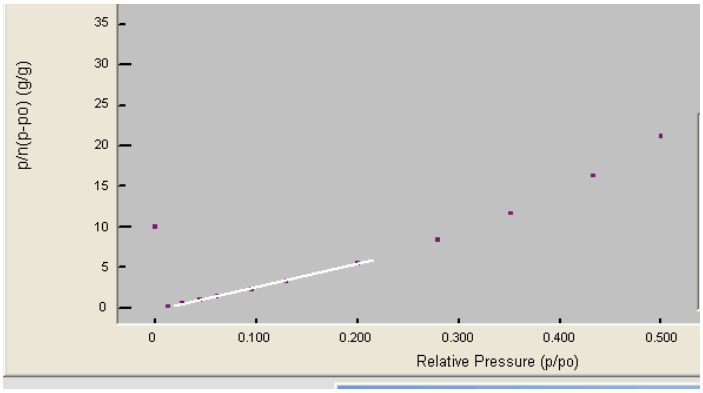

Figure S19 : Plot of the linear region for the BET equation in the range below p/p^0 0.22.

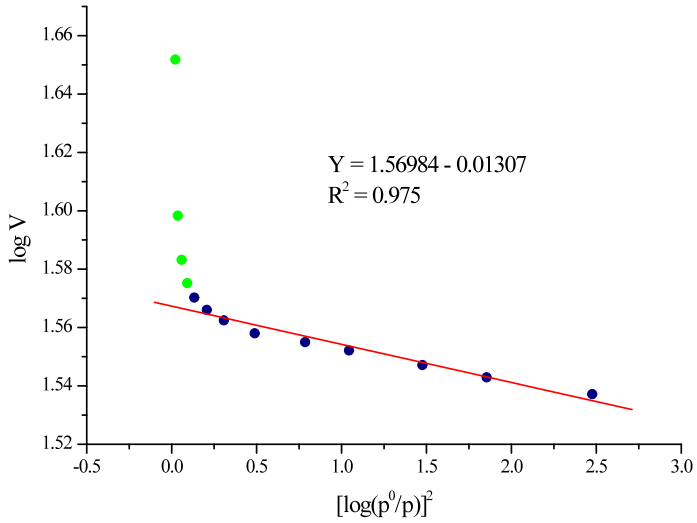

Figure S20 : Plot of DR equation (from N_2 isotherm measured at 77 K and 1 bar) of $\log V = f\,[(\log p^0/p)^2]$

Isosteric heats of adsorption

The carbon dioxide and methane affinity of this material can be quantitatively reflected by the isosteric heat of adsorption Qst, which is calculated utilizing the virial-type expression, using the adsorption branches measured at 273 K and 298 K.

$$\ln P = \ln N + \frac{1}{T}\sum_{i=0}^{m} a_i N^i + \sum_{i=0}^{n} b_i N^i$$

Where :

- P : pressure of the adsorption at T_1 = 273 K and T_2 = 298 K
- N : amount adsorbed
- T : temperature
- a_1 and b_1 : virial coefficients
- *m* and *n* : represent the number of coefficients required to describe the isotherm

The values of the virial coefficients a_0 through a_m were then used to calculate the isosteric heat of adsorption using the following expression:

$$Qst = - R\sum_{i=0}^{m} a_i N_i$$

Where :

- Qst : isosteric heat of adsorption
- R : gas constant

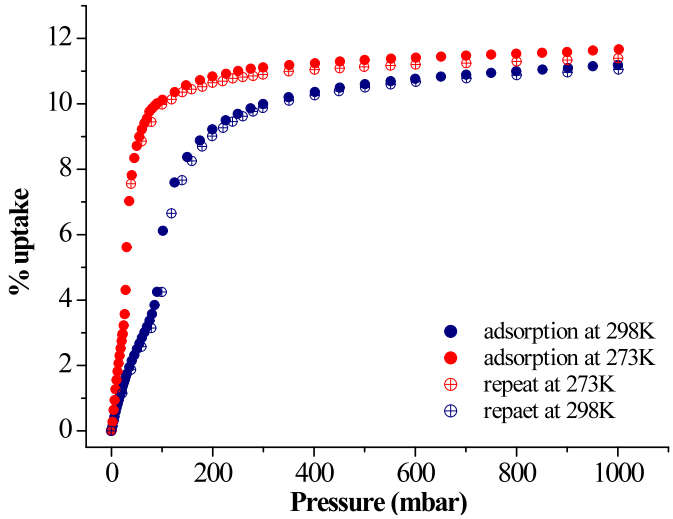

Figure S21 : CO_2 adsorption branches collected on **1′** at 1 bar and 273 K and 298 K (filled balls: high resolution CO_2 adsorption, empty balls: repeat of CO_2 adsorption in a different batch of sample).

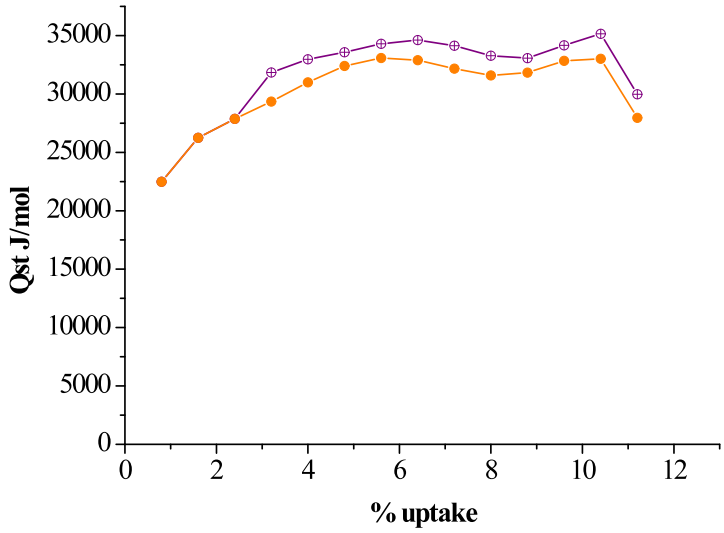

Figure S22: Isosteric heats of adsorption of **1′** as a function of CO_2 loading on a different batch of sample (see figure above – filled and empty balls).

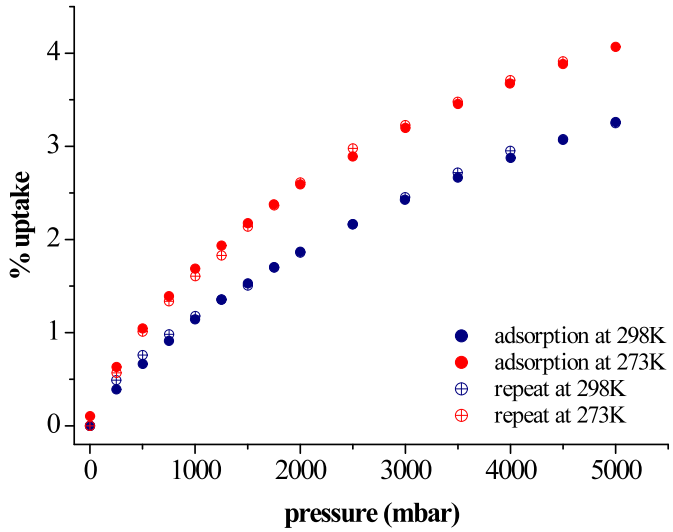

Figure S23 : CH_4 adsorption branches collected on **1′** at 5 bar and 273 K and 298 K (filled balls: CH_4 adsorption, empty balls: repeat of CH_4 adsorption on a different batch of sample).

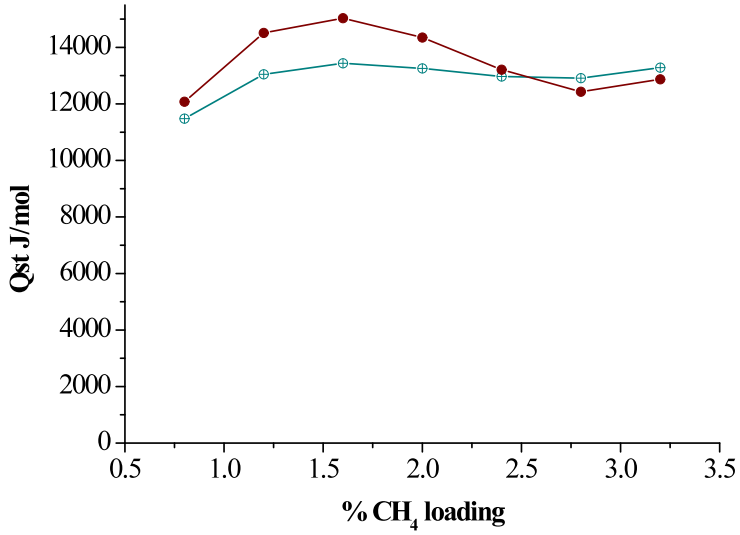

Figure S24 : Isosteric heat of adsorption of two different samples of **1′** as a function of CH_4 loading (see figure above – filled and empty balls)

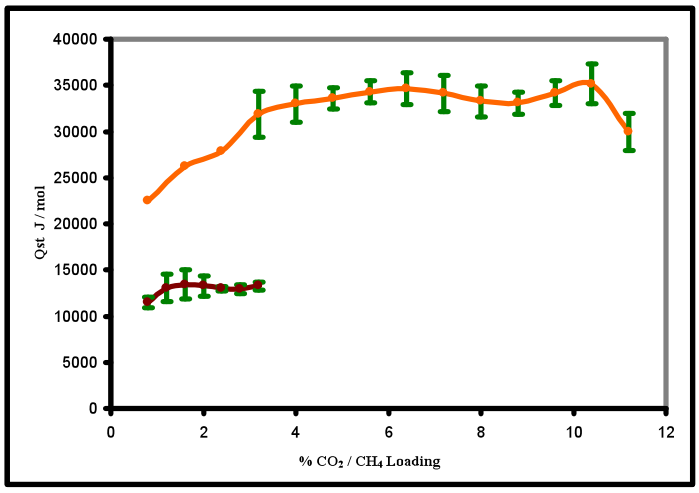

Figure S25 : Isosteric heat of adsorption of **1′** as a function of CH_4 (brown) and CO_2 (orange) loading. The error bars are the result of the standard deviation from two independent adsorption measurements.

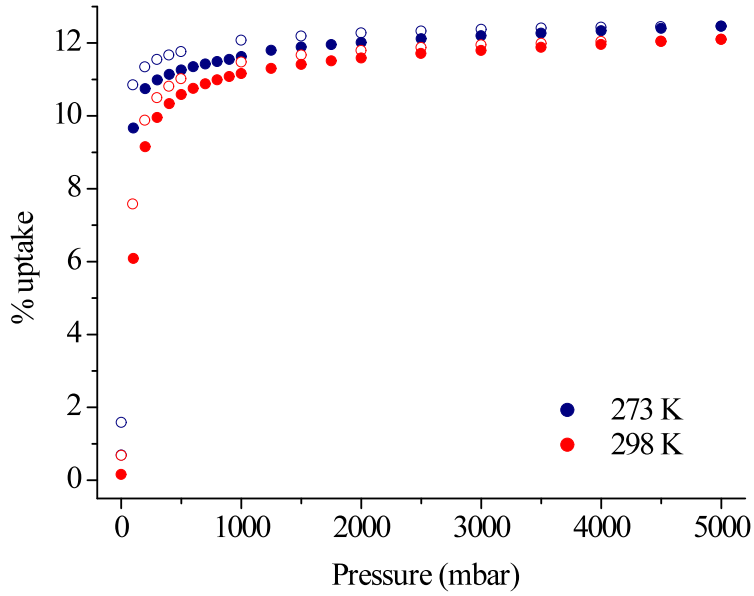

Figure S26 : CO_2 isotherms collected at 5 bar and 273 K and 298 K showing the selectivitry of **1′** to CO_2. (filled balls: adsorption and empty balls: desorption)

7. Breakthrough Experiment

Breakthrough experiments were performed using a column with a length of 18.1 cm and diameter of 0.21 cm, packed with the material. The sample was initially outgassed at 60 ºC under high vacuum (Anal. Calcd for ($[Ni_3(pzdc)_2(7Hade)_2(H_2O)_4]\cdot(H_2O)_{0.4}$) : C 28.88, H 2.52, N 23.57. Experimental: C 28.92, H 2.59, N 23.64.) The flow rates of all gases (He, CO_2 and CH_4) were regulated by mass flow controllers (0-100 ml/min). Once the outlet of the gas flow controllers was connected with the mass spectrometer (MS), the sample was reactivated in situ heating it overnight at 100 ºC under He flow (10 ml/min). The experiment was performed at 298K and atmosphere pressure. Before each experiment the sample was activated by heating it at 100 ºC for 1 hr.

8. References

1. D. Bradshaw, J. E. Warren and M. J. Rosseinsky, *Science*, 2007, **315**, 977-980
2. J. An, S. J. Geib and N. L. Rosi, *Journal of the American Chemical Society*, 2010, **132**, 38-39.
3. J. Y. An, S. J. Geib and N. L. Rosi, *Journal of the American Chemical Society*, 2009, **131**, 8376-8377.
4. J. Y. An, R. P. Fiorella, S. J. Geib and N. L. Rosi, *Journal of the American Chemical Society*, 2009, **131**, 8401-8403.
5. J. P. Garcıa-Teran, O. Castillo, A. Luque, U. Garcıa-Couceiro, P. Roman, and F. Lloret, *Inorg. Chem*. 2004, **43**, 5761-5770
6. SAINT v7.68A (Bruker, 2009)
7. TWINABS-2008/4 (Bruker, 2010)
8. Olex2 - O. V. Dolomanov, L. J. Bourhis, R. J. Gildea, J. A. K. Howard and H. Puschmann, J. *Appl. Cryst.,* 2009, **42***,* 339-341
9. Superflip – G. Oszlanyi, A. Suto, Acta Cryst., 2004, **A60**, 134-141
10. Shelxl – G. M., Sheldrick *Acta Cryst.,* 2008, **A64**, 112-122
11. Humphrey, W., Dalke, A. and Schulten, K., `VMD - Visual Molecular Dynamics', J. Molec. Graphics 1996, **14.1**, 33-38.